Cortical Spreading Depression Can Be Triggered by Sensory Stimulation in Primed Wild Type Mouse Brain: a Mechanistic Insight to Migraine Aura Generation

Sahin Hanalioglu
Hacettepe University: Hacettepe Universitesi https://orcid.org/0000-0003-4988-4938
Aslihan Taskiran-Sag
Hacettepe University: Hacettepe Universitesi
Hulya Karatas
Hacettepe University: Hacettepe Universitesi
Buket Donmez-Demir
Hacettepe University: Hacettepe Universitesi
Sinem Yilmaz-Ozcan
Hacettepe University: Hacettepe Universitesi
Emine Eren-Kocak
Hacettepe University: Hacettepe Universitesi
Yasemin Gursoy-Ozdemir
Koc University: Koc Universitesi
Turgay Dalkara (tdalkara@hacettepe.edu.tr)
Institute of Neurological Sciences and Psychiatry, Hacettepe University https://orcid.org/0000-0003-3943-7819

Research article

Keywords: cortical spreading depression, ouabain, Asante Potassium Green-4, photic stimulation, whisker stimulation, migraine

Posted Date: October 28th, 2021

DOI: https://doi.org/10.21203/rs.3.rs-1010226/v1

Version of Record: A version of this preprint was published at The Journal of Headache and Pain on August 19th, 2022. See the published version at https://doi.org/10.1186/s10194-022-01474-0.

Abstract

Background: Unlike the spontaneously appearing aura in migraineurs, experimentally, cortical spreading depression (CSD), the neurophysiological correlate of aura is induced by non-physiological stimuli. Consequently, neural mechanisms involved in spontaneous CSD generation, which may provide insight how migraine starts in an otherwise healthy brain, remains largely unclear. We hypothesized that CSD can be physiologically induced by sensory stimulation in primed mouse brain.

Methods: Cortex was made susceptible to CSD with partial inhibition of Na^+/K^+-ATPase by epidural application of a low dose of Na^+/K^+-ATPase blocker ouabain that does not induce repetitive CSDs or by knocking-down α2 subunit of Na^+/K^+-ATPase, which is crucial for K^+ and glutamate re-uptake by astrocytes, with shRNA. Stimulation-induced CSDs and extracellular K^+ changes were monitored in vivo electrophysiologically or with a K^+-sensitive fluoroprobe (IPG-4).

Results: After priming with ouabain, photic stimulation increased the CSD incidence compared with non-stimulated animals (44.0 vs. 4.9%, $p<0.001$). Whisker stimulation was less effective (14.9 vs. 2.4%, p=0.02). Knocking-down Na^+/K^+-ATPase (50% decrease in mRNA) lowered the CSD threshold in all mice tested but triggered stimulus-induced CSDs in 14.3% and 16.7% of mice with photic and whisker stimulation, respectively. Confirming Na^+/K^+-ATPase hypofunction, extracellular K^+ significantly rose during stimulation after subthreshold ouabain or shRNA treatment unlike controls. In line with higher CSD susceptibility, K^+ rise was more prominent after ouabain. To gain insight to preventive mechanisms reducing the incidence of stimulus-induced CSDs, we applied an A1-receptor (DPCPX) or GABA-A (bicuculine) antagonist over the occipital cortex, because adenosine formed during stimulation or inhibitory interneuron activity can reduce CSD susceptibility. DPCPX induced CSDs or CSD-like small-DC shifts during photic stimulation, whereas bicuculine was not effective.

Conclusions: Our findings indicate that normal brain is well protected against CSD generation. For CSD to be ignited under physiological conditions, priming and predisposing factors are required as seen in migraine patients. Intense sensory stimulation has the potential to trigger a CSD when co-existing conditions can bring extracellular K^+ and glutamate concentrations over threshold via reduced uptake of K^+ and glutamate (e.g. inefficient fueling of α2-Na^+/K^+-ATPase due to reduced glycogen breakdown) or facilitated glutamate release (e.g. reduced presynaptic adenosinergic inhibition).

Background

Cortical spreading depression (CSD) is regarded as the neurophysiological correlate of migraine aura and as a potential trigger for migraine headache [1]. CSD is a slowly propagating depolarization wave that spreads through the gray matter by depressing electrical activity. CSD is induced by various methods in experimental animals to study the pathophysiology of migraine aura and headache [1–3]. These methods involve direct stimulation of the exposed brain tissue with electrical, mechanical (pinprick) or chemical (e.g. KCl, glutamate) stimuli. Recently, optogenetic methods made a relatively non-invasive CSD

induction possible [4]. Although CSDs induced by any of these methods share similar characteristics with spontaneously occurring CSDs and have been instrumental to investigate the electrophysiological characteristics of CSD, associated blood flow changes and headache generating mechanisms, the tools used are yet non-physiological unlike the conditions spontaneously generating CSDs (auras) in patients. Therefore, experimental methods that mimic the human condition more closely are needed to understand the mechanisms generating CSD in migraineurs' normally functioning brain, a crucial but very underexplored step in migraine pathophysiology.

We hypothesized that CSD could be non-invasively evoked by intense sensory stimulation in the mouse brain because migraine headaches can be triggered by intense light or auditory stimulation as well as exercise [5–8]. Since these physiological triggers can initiate migraine aura and headache in genetically or hormonally primed migraineur brain but generally not in the non-migraineurs, we tested the effect of intense sensory stimulation on the mouse brain made susceptible to CSD by partial inhibition of Na^+/K^+-ATPase with low concentrations of ouabain or by knocking-down its α2 subunit. Ouabain application to the brain tissue is well known to induce repetitive CSDs [9]. However, its sub- or around-the-threshold doses can predispose to CSD generation without triggering CSDs similar to the familial hemiplegic migraine type 2 (FHM2) patients having haploinsufficiency of ATP1A2 gene that encodes α2 subunit of Na^+/K^+-ATPase [10]. These patients have a normal brain function but are prone to occasional hemiplegic migraine with aura attacks. Like patients with FHM2, the knock-in mice bearing the human FHM2 mutation do not develop spontaneous CSDs but has a lower threshold for CSD generation induced by electrical or KCl stimulation [11, 12]. Hence, to more specifically test the role of Na^+/K^+-ATPase inhibition in priming the cortex to CSD, we selectively knocked-down α2-Na^+/K^+-ATPase expression in the cortex by RNA interference in addition to the ouabain experiments. We chose α2-Na^+/K^+-ATPase as a target because it plays a significant role in removing K^+ and glutamate released during excitatory synaptic activity [13–15]. We have found that both approaches consistently lowered the CSD threshold and, importantly, photic or whisker stimulation elicited CSDs in the cortex primed by these approaches. We also found that for CSD to be ignited, mechanisms preventing neuronal synchronization (e.g. adenosine generated by synaptic activity) must be outcompeted.

Methods

Animals

All animal experiments were performed in accordance with relevant guidelines and regulations, and were approved by Hacettepe University Animal Experiments Ethics Committee (2012/53-01, 2017/05-2). A total of 140 male and female Swiss albino mice (25 to 35 g) were used. All mice were housed with ad libitum access to food and water under a fixed 12-hour light/12-hour dark cycle.

Anesthesia

Mice were anesthetized with intraperitoneal injection of xylazine (10 mg/kg) and urethane (1.25 g/kg), which suppresses cortical excitability relatively less compared to commonly used anesthetics like isoflurane and ketamine [16, 17]. After maintaining an adequate depth of anesthesia, mice were positioned prone and fixed in stereotaxic frame (Digital Lab Standard Stereotaxic Frame, Stoelting, USA). In photic stimulation experiments, eyes were covered by lubricant gel and eyelids were closed with surgical clips to avoid corneal drying and enhance cortical sensitivity to light [18]. The heart rate and tissue oxygen saturation were continuously monitored by a pulse oximeter (V3304 Digital Table-Top Pulse Oxymeter, Nonin, USA) throughout all experiments. 100% oxygen mixed with room air (2 l/min) was delivered to the spontaneously breathing mice to avoid hypoxia. Rectal temperature was maintained at 37.0±0.2°C using a homeothermic blanket (Harvard Apparatus, UK) for the duration of the experiment. The depth of anesthesia was checked with toe/tail pinch and/or eye blink reflex at 10-15 minute intervals and additional doses of anesthetics were injected when needed. Animals with persistent hemodynamic instability or hypoxia were excluded from the study.

Surgery

A midline incision was made over the scalp to expose the skull. One or two small circular areas (diameter<1 mm) were thinned with a high-speed drill (WPI, USA) to house the electrode tips over the cranium covering the right hemisphere; one at the anterior parietal and the other one at the frontal region. During drilling process, the skull was continuously irrigated with cold saline to prevent thermal injury to the underlying cortex.

A cranial window (2 mm in diameter) was opened over the cranium covering either the visual cortex (for photic stimulation) or somatosensory barrel cortex (for whisker stimulation) without damaging the underlying dura mater. In a subset of experiments, a plastic cylindrical tube (inner diameter and height, 2 mm) was placed over the exposed intact dura and fixed to the skull by dental acrylic to encircle the cranial window. This chamber allowed topical administration of ouabain or the fluorescent potassium probe (Asante Potassium Green-4) as well as fluorescent imaging.

Photic and Whisker Stimulation

A custom-made photic stimulator was used to illuminate both eyes. The frequency, intensity, duration and pattern of the stimulation were adjustable using a stimulus isolator (World Precision Instruments A385, USA) and a computer interface (LabChart, AD Instruments, Australia). 5-mm, 2V white mini-LED bulbs were used for stimulation. The LEDs were mounted on flexible arms that allowed optimal positioning of the LEDs for each individual mouse in stereotaxic frame.

Whiskers were cut to 1 cm and automatically stimulated by using a custom-made apparatus. This device allowed stimulation of the whiskers unilaterally with a tip blunted watercolor brush (no:8) in vertical plane at an adjustable frequency (4 to 30 Hz) without touching common fur or other parts of the face of the mouse placed in the stereotaxic frame.

Laser Speckle Contrast Imaging

Cerebral blood flow (CBF) changes were detected with laser speckle contrast imaging as described before [19]. Briefly, the region of interest was illuminated with a 785-nm laser diode (Thorlabs DL7140-201, Thorlabs, USA) and imaged under 4X magnification by using a stereomicroscope (Nikon SMZ 1000, Nikon, Japan) and a charge-coupled device camera (Basler 602F, Basler Vision Technologies, Germany). Consecutive raw speckle images were acquired at 100 Hz (an image set) at 1-second intervals, processed by computing the speckle contrast using a sliding grid of 7x7 pixels, and averaged to improve the signal-to-noise ratio. Speckle contrast images were converted to images of correlation time values, which are inversely and linearly proportional to the mean blood velocity. Image J 1.42 software (NIH, USA) was used to compute and pseudo-color the relative blood flow changes in the cortex after sensory stimulation compared to baseline values.

Epifluorescence Microscopy

In a subset of experiments, fluorescent-tagged ouabain (BODIPLY® FL Ouabain, Molecular Probes, USA) was topically applied over the dura by a cotton ball soaked with 5 µl of 0.1 mM ouabain in saline. Animals were sacrificed and the brains were removed after 60 minutes. 20 µm-thick coronal sections were obtained from the frozen brains. Sections were cover-slipped with Hoechst-33258 to delineate the tissue architecture by staining cell nuclei and, imaged under a fluorescence microscope using appropriate filter sets to assess the penetration and diffusion of ouabain into the brain tissue. In preliminary experiments (n=3 mice), we also evaluated the distribution of fluorescent-tagged ouabain after intracerebroventricular (icv) administration (5 µL, 100 µM) to see whether this route could provide sufficient concentrations in the cortex. However, 45 minutes after intracerebroventricular administration ouabain, only accumulated in the vicinity (around 100 µm) of the ventricle and did not diffuse to cortex so, this route of administration was not preferred.

Electrophysiology

To record the DC potentials, one or two Ag/AgCl pellet electrodes (E205, 1 mm diameter, Warner Instruments, USA) were placed and fixed over the thinned skull as described above. The electrode tips were covered with EEG electrode gel to enhance the electrical contact with the cranial bone. A disc-shaped Ag-AgCl ground electrode (E242, 4 mm diameter, Warner Instruments, USA) was placed between the neck muscles. The signals were digitized and acquired at 1 Hz sampling rate, displayed and analyzed by PowerLab 16/35 data acquisition system (AD Instruments).

CSD induction with sensory stimulation

For investigating the temporal relationship between the photic stimulation and CSD induction, an intermittent stimulation protocol was preferred to avoid desensitization to light. Furthermore, the room was kept dark and the eyelids were closed starting with induction of anesthesia until the stimulation in order to increase light sensitivity of the visual cortex [18]. Around-the-threshold concentration (0.1 mM) of

ouabain was topically applied over the visual cortex to prime it for CSD generation. Following a 30-minute CSD-free silent period in these mice, the eyes were opened and 1-minute on-off cycles of photic stimulation (8-12 Hz) were started until a CSD was evoked or for a maximum duration of 10 minutes (5 cycles). If no CSDs were evoked, then the same stimulation pattern was repeated 10 min after the last stimulus. In case of CSD generation, the next stimulation was initiated after a 30-min silent period has passed. Eyes were closed again right after a CSD was evoked until the next stimulation or during the 10-min pauses between the photic stimulation epochs. The experiment was terminated in 5 mice (out of 22) if the experiment duration exceeded 4 hours (n=2) or repetitive CSDs were observed during 2-hour recording without a 30-min silent period between them (n=2) or the animal was hemodynamically unstable (n=1). The effect of photic stimulation on a group of α2-Na^+/K^+-ATPase knockdown mice was also evaluated with the same protocol.

Whisker stimulation experiments were carried out with the same protocol to the one applied for photic stimulation. For these experiments, ouabain soaked cotton ball was placed over the somatosensory barrel cortex and only female mice were used to increase the CSD susceptibility because their CSD threshold is lower [20]. Contralateral whiskers were stimulated as detailed above. The effect of whisker stimulation on a group of α2-Na^+/K^+-ATPase knockdown mice was also evaluated with the same protocol.

α2-Na^+/K^+-ATPase knockdown

pLL 3.7 plasmid expressing α2-Na^+/K^+-ATPase-shRNA was kindly provided by Dr. Gilbert Gallardo (Washington University, School of Medicine). α2-Na^+/K^+-ATPase-shRNA consists of 21-nucleotide inverse repeats (sense sequence: 5'-GTG GCA AGA AGA AAC AGA AAC-3') separated by a 9-nucleotide loop sequence (CAAGTTAAC). The shRNA construct in the vector was verified before use by sequencing. We used empty pLL 3.7 plasmid as a control. A total of 24 mice injected with shRNA and 9 mice with control blank plasmid.

α2-Na^+/K^+-ATPase-shRNA expressing plasmid or control plasmid (1 μg) was mixed with 0.12 μl in vivo-JetPEI-TM (Polyplus transfection, France) transfection reagent. Then 1 μl of this mixture was injected at two different points intracortically 1 mm deep at a rate of 0.1 μl/min under isoflurane anesthesia by a 26 gauge Hamilton syringe. The needle was kept at the injection site for 1-minute and removed slowly over 5 minutes to allow diffusion of the plasmids into cortical layers. The sites of injection in the CSD threshold (n=6/group) and photic stimulation experiments were in the right visual cortex; (-3, 1.5) mm and (-3, 3.5) mm relative to bregma (anteroposterior and lateral coordinates, respectively) (n=6). In whisker stimulation and K^+ fluoroprobe imaging experiments, the sites of injection were in the right barrel cortex; (-0.5, 3.5) mm and (-1.8, 3) mm relative to bregma (n=6).

To verify knockdown with qRT-PCR, mice were sacrificed at 6, 24 and 48 hours after shRNA delivery. The injection areas and the contralateral homologous areas were removed and RNAs were extracted with RNeasy Mini Kit (QIAGEN, GERMANY, cat no: 74104) according to instructions. Eluted RNAs were stored

at -80°C. cDNA synthesis was performed with random hexamer primers with RevertAid First Strand cDNA Synthesis Kit (Thermo Fisher Scientific, USA cat no: K1621) according to instructions. cDNAs were stored at -20°C. qRT-PCR was performed with Taqman probe based technology. Taqman gene expression master mix (ABI, USA cat no: 4369016), FAM-MGB labeled Taqman probes for mouse ATP1A2 gene (Assay ID: Mm00617899_m1) and mouse GAPDH gene (Assay ID: Mm9999991) were used. cDNAs were diluted to 1:32 ratio in nuclease free water. The PCR was carried out in triplicates in ABI OneStep Q RT PCR machine (ABI, USA). The relative expression values were calculated with ΔΔCt method.

Detection of CSD threshold

To investigate the CSD threshold after knockdown, plasmid injected animals were tested either at 6 h, 24 h, or 48 h after injection. Increasing concentrations of KCl-adsorbed cotton balls were consecutively applied epidurally through the burr hole over the parietal bone. Each cotton ball was allowed to stay for 5 min. The DC potential was continuously recorded over the right visual cortex and the cotton ball was replaced with the next higher concentration if no CSD wave was observed during 5 min. Concentrations of KCl starting from 0.05 M and increasing by 0.025 M at each step were used to detect the threshold. Once CSD was induced, the experiment was ended. The minimum concentration that yielded the first CSD was accepted as the threshold.

Monitoring extracellular K^+ *in vivo* with a fluoroprobe

In order to investigate the extracellular potassium changes, a fluorescent potassium probe, Asante Potassium Green-4 (IPG-4, formerly APG-4, TefLABs, USA) was used. IPG-4 has a higher selectivity for K^+ over Na^+ than previous Asante potassium dyes used *in vivo*.[21] IPG-4 was prepared in 2% DMSO and diluted in artificial cerebrospinal fluid (aCSF) to yield a final concentration of 250 μM. Since it was poorly soluble in aqueous media, ultrasonic bath and gentle heating was applied to increase its solubility on the day of each experiment.

Before using for stimulation experiments, the potassium selectivity of IPG-4 was characterized in order to assess its compatibility with the large ionic shifts during CSD. For this, we applied three different concentrations of K^+ (0, 10, 50 mM) in the presence of high Na^+ concentrations in distilled water. Fluorescence intensity showed gradual increase with rising concentrations of K^+ and was similar in the presence of 77 mM or 154 mM Na^+ in the medium. Next, we investigated the distribution of IPG-4 in the mouse brain following icv (n=2) injection or topical epidural application (n=3) under an upright fluorescent microscope. Following icv injection, dye was largely accumulated in the periventricular area and did not reach the cortex. However, after topical application through a chamber over the exposed dura, IPG-4 diffused into superficial cortical layers down to 200 μm, which was satisfactory because fluorescence microscopy is limited to image only the superficial 50-70 μm of the cortex *in vivo*. Therefore, the epidural application was used for intravital imaging of extracellular potassium dynamics in the cortex.

To detect the extracellular K^+ change *in vivo*, a baseline image was captured for obtaining autofluorescence intensity of the tissue and the closed cranial chamber was filled with 8-10 µl of 250 µM IPG-4. The room was darkened during 30-min dye incubation. Then the dye was removed and the chamber was gently rinsed with aCSF three times at 37°C. Chamber was filled completely with aCSF to avoid any air bubble formation and closed by a clean cover glass for optimal fluorescence microscopy. The images were acquired under a Nikon SMZ 1000 stereomicroscope with a fluorescent attachment by using a CCD camera (Nikon DS-Qi1Mc, Japan) and NIS Elements Advanced Research Software v3.2. We used a fluorescence filter (HQ FITC LP) with excitation: 480/40 and emission: >510 nm, an exposure time of 250 ms and a signal averaging of (4x) for acquisition. Each imaging session lasted 7 minutes. Time-lapse recording for every 5 seconds started 1 min before whisker stimulation, continued through the 5 min of stimulation and ended 1 min after.

For the analysis of IPG-4 fluorescence, an ROI was placed in a predefined area that showed the maximum hyperemic response with whisker stimulation in preliminary experiments. The mean fluorescent intensity of the baseline image was subtracted from the time series images. A rolling average by 10 was applied to the image sequence. By using the *time measurement* feature of Nikon NIS-AR software, we acquired a set of signal intensity values for each session of whisker stimulation. This data set was exported for further processing and calculations to MATLAB (Mathworks, USA) software. In MATLAB (Mathworks, USA), the baseline drift that frequently accompanied the IPG-4 fluorescence was corrected by *detrending* and then the percent change from baseline (dF/F_0 %) was calculated. To incorporate both the duration and the amplitude of stimulation-induced signal change into analysis, we calculated area-under-curve (AUC) and compared AUC between groups.

Chemicals

Ouabain octahidrate (Sigma-Aldrich, USA), a Na^+/K^+-ATPase inhibitor, was topically applied with a micropipette at a total volume of 5 µL in saline either onto the cotton ball placed over the intact dura or, for IPG-4 experiments, into the cranial window. Electrophysiological recordings were started before ouabain applications and continued 150 minutes to monitor CSD occurrence. To determine the threshold dose for CSD induction, ouabain solutions at different concentrations (0.05, 0.1, 0.15, 0.3, 0.5 mM) were tested. The time to CSD induction and CSD frequency were measured for each tested concentration in a fixed volume (5 µl).

8-Cyclopentyl-1,3-dipropylxanthine (DPCPX, Tocris, UK), a high affinity adenosine A1 receptor selective antagonist, was dissolved in DMSO as a stock solution (30 mM). On the day of each experiment, the drug was suspended in saline and gently heated at a concentration of 30 µM for intracortical injection or 0.7-1 mM for epidural application with a cotton ball.

(+)Bicuculline (Tocris, UK), a competitive antagonist of GABAA receptors, was dissolved in 1% DMSO at a concentration of 5-10 mM and applied epidurally with a cotton ball.

Statistics

Data were presented as mean ± SE or median (range) or percentage (%) of the total and were analyzed using chi-square test or Mann-Whitney U test, where appropriate. To differentiate sensory stimulation induced CSDs from spontaneously occurring CSDs, a modified version of the method previously used by von Bornstadt et al. was adopted [22]. The statistical method used to analyze each dataset is indicated in respective figure legends.

Results

Detecting around-the-threshold dose of ouabain for CSD induction

No CSD was induced with 0.01 and 0.05 mM concentrations of ouabain topically applied over the cortex for 150 min, whereas repetitive CSDs were evoked (≥5 CSDs within 150 min) with 0.3 mM (n=4) or 1 mM (n=4) (Table 1). With 0.1 mM ouabain (n=16), no CSD was evoked in 25%, 1-2 CSDs in 50% (38 and 12%, respectively) and ≥5 CSDs were detected within 150 min in only 25% of the experiments, whereas more than 5 CSDs were recorded in 52% of experiments with 0.15 mM (n=25) (Table 1). The mean latency to the first CSD was short with 0.3 and 1 mM ouabain (21±5.6 and 13±2.5 min), in contrast, it was significantly delayed with 0.1 mM (46±4.4 min) concentration (p=0.001) (Table 1). Therefore, 0.1 mM ouabain was chosen as around-the-threshold concentration and used for creating susceptibility to CSD in sensory stimulation experiments because the probability of repetitive CSD induction was low and had considerable latency.

Optimization of Photic and Whisker stimulation

In order to determine the optimal sensory stimulation parameters and accurate mapping of respective sensory cortices, regional CBF changes were measured following photic or whisker stimulations on occipital and barrel cortices, respectively. Maximal CBF changes at visual cortex were observed with 8-12 Hz photic stimulation in preliminary experiments (n=3 mice). The peak increase in CBF at these frequencies was 11.9±2.1%, whereas the mean CBF change during the stimulation period was 7.6±1.7%. The CBF increase reached a maximum within 15-30 seconds followed by a plateau during the stimulation and rapid decline to baseline after the stimulation. The slope of the plateau was about zero for 1-min stimulation period while it turned negative in longer duration of stimulations, possibly representing adaptation of visual cortex to continuous stimulation. Accordingly, 1-min stimulation period was chosen for the visual stimulation experiments.

Maximal CBF changes at the somatosensory barrel cortex were observed with whisker stimulation at 12-20 Hz. The peak CBF change for these frequencies was 12.4±3.3%, whereas the mean CBF change during stimulation period was 5.1±1.4% (n=3 mice). The CBF increase reached a maximum within 30-60 seconds followed by a plateau during the stimulation and declined to baseline within 15-20 seconds after the stimulation. The slope of the plateau was about zero up to 10-min stimulation periods. Accordingly, whisker stimulation was continued for 5 and occasionally 10 mins.

CSD induction with photic stimulation in pharmacologically primed mouse visual cortex

With intermittent photic stimulation of the ouabain-primed visual cortex, a strong probable relationship was found between the photic stimulation and CSD occurrence in 9 of 15 animals tested (60%)(Figure 1, 2). A total of 16 CSDs were recorded during or just after 1-min photic stimulation pulse following a 30-min CSD free priming (“silent”) period with 0.1 mM ouabain. The time elapsed between the start of photic stimulation cycles and the CSD generation was 4.1 ± 1.0 min on average but was quite variable ranging from 20 secs (i.e. with the first pulse of stimulation) to 10 mins (i.e. with the last 1-min pulse). To prove that the observed CSDs were indeed triggered by photic stimulation, we tested whether or not the incidence of CSDs following photic stimulation differs from that of the spontaneously emerging (“non-stimulated”) CSDs after priming with around-the-threshold concentration of ouabain but without photic stimulation. A probabilistic approach previously used by von Bornstadt et al. was adopted to test this possibility. The average non-stimulated CSD incidence calculated by measuring the chance of CSD occurrence for each 10-min epochs (total stimulus duration) following a 30-min silent phase was found to be 4.8%. However, the average incidence of CSDs after photic stimulation was 44%, which was significantly higher compared to the stimulus-independent CSD incidence ($p<0.001$).

CSD induction with whisker stimulation in pharmacologically primed mouse barrel cortex

In a different set of experiments, a similar experimental protocol resulted in CSD induction following whisker stimulation in 5 of 11 mice tested (45.5%)(Figure 3). A total of seven CSDs associated with stimulation were recorded in those five animals. The duration between the start of whisker stimulation and the CSD generation was 2.8±0.6 min on average but was quite variable ranging from 20 sec (i.e. at the beginning of the first 5-min pulse) to 8 mins (i.e. during the second pulse). Average incidence of CSDs for each 5-min periods corresponding to duration of whisker stimulation was 14.9%, while it was only 2.4% for CSDs emerging without whisker stimulation ($p=0.02$).

Distribution of BODIPY-ouabain in the mouse brain

To evaluate the distribution of ouabain in the mouse brain after focal epidural administration, we applied fluorescent-labeled ouabain (BODIPY-ouabain) at the same dose (5 µl, 100 µM) and manner as used in priming experiments. Mice (n=3) were sacrificed 45 min after the drug administration and brain sections were evaluated under fluorescence microscope. Ouabain was largely accumulated in dura mater and the underlying superficial cortical layers. The signal intensity steeply declined as the drug penetrated into deep cortical layers. Beyond 140.6±13.4 µm depth, fluorescent signal was barely detectable (<1% of maximum intensity detected in more superficial layers). Longitudinally, fluorescence signal was restricted to cranial window area with no significant lateral spread beyond its borders.

Susceptibility to CSD after partially silencing α2-Na^+/K^+-ATPase expression

We validated α2-Na^+/K^+-ATPase knockdown by qRT-PCR and found a 50 % decrease in α2-Na^+/K^+-ATPase mRNA levels in the occipital cortex injected with α2-Na^+/K^+-ATPase-shRNA compared to the control group (n=3 mice/group) (Figure 4). Intracortical knockdown of α2-Na^+/K^+-ATPase led to a decrease in the CSD threshold at 6 (n=3) and 24 (n=3) hours following injection of the plasmid (median=

0.1 M KCl vs 0.175 M KCl in α2-Na^+/K^+-ATPase-shRNA injected and blank plasmid injected controls (n=6), respectively; p=0.002)(Figure 4). No spontaneous CSDs were observed in these mice during 8±2 min monitoring before induction with KCl. In another set of α2-Na^+/K^+-ATPase knockdown mice, photic stimulation induced CSDs in 1 out of 7 mice 24 h after injection, whereas whisker stimulation triggered CSDs in 1 out of 6 mice. Two additional α2-Na^+/K^+-ATPase knockdown mice were recurrently tested with photic cycles at 6 h, 24 h and 48 h (under brief isoflurane anesthesia on each day) not to miss any effective time point; however, we did not observe CSD at any time point, altogether suggesting that the probability of CSD induction by sensory stimulation is low after partial α2-Na^+/K^+-ATPase knockdown despite consistently reduced CSD threshold in these mice. This could be explained by a below the threshold rise in K^+ due to a reduced uptake during stimulation for CSD generation, which is only exceeded when supplemented with exogenous KCl as in the threshold experiments in line with a recent study on brain slices obtained from heterozygous α2-Na^+/K^+-ATPase knockout mice [23].

Extracellular potassium changes during sensory stimulation

To assess whether or not ouabain or α2-Na^+/K^+-ATPase knockdown did effectively reduce K^+ uptake, we monitored the extracellular potassium change during intense whisker stimulation by plotting the relative fluorescence intensity change (dF/F_0) over time and calculating the area under the curve (AUC). In ouabain-primed (0.1 mM) mice, 5 min of 10 Hz whisker stimulation resulted in a significant increase in K^+ fluorescence compared to aCSF-treated control group (n=6 mice for each group, 323 ± 68 vs. 74 ± 19 dF/F_0%.sec, p=0.004) (Figure 5A). Similarly, there was significant increase in potassium signal during whisker stimulation in α2-Na^+/K^+-ATPase shRNA-encoding plasmid injected mice compared to blank plasmid injected animals (118 ± 35 vs. 25 ± 24 dF/F_0%.sec, p=0.055), however, to a notably lesser degree than ouabain induced rise as also suggested by sensory stimulation experiments with these mice (Figure 5B).

Whisker stimulation induced CSDs in 1 out of 6 knockdown mice as indicated above, which was excluded from the analysis because a marked increase in fluorescent intensity coincident with an electrophysiologically recorded DC shift was observed. The increased K^+ signal propagated at a speed of 1.5 mm/min) in accordance with a spreading CSD.

Breaking mechanisms reduce CSD incidence

Priming the mouse brain by targeting Na^+/K^+-ATPase increased the probability of CSD generation with sensory stimulation. However, its probabilistic nature suggested presence of braking mechanisms that prevent full-blown CSD ignition. We hypothesized that adenosine generated during prolonged synaptic activity by breakdown of ATP could decrease glutamate release from thalamocortical nerve endings and, hence, counteract the drive for CSD ignition. This can be one of the several safety mechanisms that prevent CSDs in the normal brain. To test this hypothesis, we used a selective A1-receptor antagonist (DPCPX) to reduce the adenosinergic inhibition on glutamate release and postsynaptic excitability.

DPCPX was applied to the non-primed occipital cortex epidurally (0.7-1 mM) in 5 mice and intracortically (30 µM, 200 µm deep)[24] in 3 additional mice without any notable differences in the results. In 4 of these mice, DPCPX application over dura caused 6 full-blown CSDs before stimulation (Figure 6). When DPCPX concentration was below the threshold to ignite full-blown CSDs, photic stimulation (116 sessions in 6 mice) induced 10 small-DC shifts (coincident with EEG suppression) having a similar duration to CSDs with mean amplitude of 1.4 ± 0.2 mV and duration at half maximum of 90±17 sec. Of note, since the recordings were made over the skull without opening a burr hole to maintain the cortical physiology intact at the recording site, the amplitudes are smaller compared to the intracortically recorded CSDs. So, we normalized the amplitude of small-DC shifts to the pinprick-induced full-blown CSDs at the end of the experiment, which was 17.3 ± 1.8 % to assess their magnitude relative to full-blown CSDs. Because of the poor solubility of DPCPX like most other A1 antagonists and rapid absorption of its solvent DMSO through the dura underlying the cranial window during prolonged application, a precise control over the concentration achieved in cortex was not possible, hence, combination experiments with ouabain or dose-response experiments for detecting the thresholds of full-blown CSD and small-DC shift were not feasible. Systemic administration was also not possible because of cardiac arrhythmia.

Some of the thalamocortical sensory fibers terminate on feed-forward GABAergic inhibitory neurons that prevent overexcitation of cortical pyramidal neurons by sensory input. Accordingly, we tested whether or not this (and other forms of) GABAergic inhibition also contributed to the braking mechanism. In 6 mice, we applied bicuculine epidurally over the occipital cortex. In none of these mice except one, photic stimulation induced no appreciable DC shifts unlike DPCPX. In one mouse, however, a full-blown CSD was generated during photic stimulation (Figure 6E). Both DPCPX and bicuculine were not completely dissolvable in DMSO, so, we ensured that they penetrated cortex by observing appearance of irregularly spaced synchronized discharges (Figure 6A, D).

Discussion

CSD is considered as the fundamental intrinsic brain event underlying migraine aura and leading to cascades of parenchymal and meningeal inflammatory signaling that result in headache [1, 25–27]. In this study, we have shown that intense sensory stimulation, one of the triggers inducing migraine with aura, can indeed generate CSD in the mouse brain primed by reducing K^+, hence glutamate, uptake (see below paragraph) with pharmacological or genetic means. Therefore, migraine triggers (e.g. sleep deprivation [28]) can predispose to CSD and migraine attack by lowering the capacity for K^+ and glutamate uptake during intense sensory stimulation. However, for realization of CSD ignition, intrinsic mechanisms preventing neuronal synchronization (e.g. adenosine generated during synaptic activity) must also be overcome.

Pharmacological sensitization with ouabain

Ouabain is a digitalis derivative that blocks Na^+-K^+-ATPase ion pump on cell membranes. At concentrations that inhibit a large fraction of α1 as well as α2 and α3 isoforms of Na^+/K^+-ATPase in

cortical and hippocampal slices *in vitro*, ouabain induces spreading depolarizations characterized by incomplete repolarization similar to that of anoxic depolarization [1, 9]. This shows that repolarization phase of the DC potential shift mainly reflects K^+ reuptake and restoration of the transmembrane K^+ gradient by Na^+/K^+-ATPase pump. Indeed, partial inhibition of α1-isoform in hippocampal slices allows restoration of the resting membrane potential, hence, the repolarizing phase of CSD and, leads to prolonged negative DC shifts depending on the degree of blockade of α1 subunit of Na^+/K^+-ATPase [9, 29]. However, lower concentrations of ouabain preferentially inhibit the α2 isoform expressed on peri-synaptic astrocyte processes that plays an important role in clearance of limited amounts of K^+ and glutamate released during synaptic activity [9, 13, 14]. Rises in extracellular glutamate and K^+ are known to trigger CSD.[1–3] The CSDs we observed after topical ouabain priming had a complete and fast repolarization phase and were similar to CSDs induced by K^+ application or pin-prick, suggesting that the concentrations of ouabain used in our study may have preferentially blocked astrocytic α2 and neuronal α3 isoforms but not significantly the α1 isoform [23], which has a thousand times lower affinity to ouabain compared to the other isoforms [30]. Imaging with fluorescent-labeled ouabain demonstrated that epidurally applied ouabain diffuses down only to the first layers of cortex with a steeply decreasing concentration toward the 2-4th layers where the apical dendrites generating the CSD are located, suggesting that we were able to adjust the ouabain concentration to mainly inhibit the α2/α3 isoforms in these layers. Similar to our approach, Calderon et al. was able to mimic rapid-onset dystonia and Parkinsonism caused by a genetic defect in α3 isoform of Na^+/K^+-ATPase by infusing low doses of ouabain (18 ng/h) into basal ganglia and cerebellum of the wild type mice [31]. Our extracellular K^+ measurements with a fluoroprobe confirmed that the concentration of ouabain applied inhibited α2 isoform, leading to a measurable rise in extracellular K^+ during prolonged sensory stimulation (i.e. synaptic activity), which can potentially exceed the threshold to ignite CSD. A study on brain slices showed that rising extracellular K^+ concentration up to 15 mM in a cortical volume of as small as 0.03-0.06 mm^3 was sufficient to trigger a CSD [32]. Such a concentration is likely to be attained within the minute volume of interstitium around synapses when K^+ uptake during intense excitatory synaptic activity is slowed down. Under the same conditions, glutamate uptake by astrocyte processes is also suppressed as the Na^+ gradient driving glutamate transporters is maintained by α2-Na^+/K^+-ATPase; thus, both proteins are intimately co-localized at the membrane of processes [14, 33–35]. Indeed, ouabain as well as FHM2 mutations have been shown to significantly slow down the decay kinetics of glutamate signal at various stimulation intensities in the somatosensory cortex [36, 37]. Inhibition of α3 isoform might potentially facilitate CSD induction by partially depolarizing neurons although observations from brain slices suggest the contrary [23]. However, unlike D801N α3-Na^+/K^+-ATPase knock-in mouse that has a dysfunctional α3 subunit, we did not observe hyperexcitable responses to sensory stimulation and prolonged CSDs with our ouabain application protocol [38]. We should note that our aim was essentially to create susceptibility to CSD with ouabain rather than investigating the isoform involved in sensory stimulation triggered CSDs. However, our data, albeit indirectly, favor α2-Na^+/K^+-ATPase over other isoforms as the main target of low concentration of ouabain we used. This also conforms to human

genetic data; mutations in ATP1A1 and 3 cause more severe phenotypes like seizures unlike most mutations in ATP1A2 [39, 40].

Sensitization with α2-Na^+/K^+-ATPase knockdown

To specifically assess the role of α2 subunit of Na^+/K^+-ATPase pump in CSD susceptibility *in vivo*, we knocked down its expression by RNA interference, which yielded a 50 % decrease in α2-Na^+/K^+-ATPase mRNA in the cortex. This approach indeed lowered the CSD threshold in line with the observations from FHM2 knock-in mice: Capuani et al. showed that defective glutamate and potassium clearance by cortical astrocytes underlies the CSD susceptibility in W887R knock-in mice due to the reduced expression of astrocytic α2 isoform of Na^+/K^+-ATPase [33]. G301R FHM2 knock-in mouse had a more severe phenotype; in addition to lowered CSD threshold, their CSD duration was prolonged unlike W887R knock-in mice [12]. Unfortunately, for a fine control, the RNA interference experiments were inherently not as flexible to further lower the pump activity as was pharmacological inhibition with ouabain, in which we could have adjusted around-the-threshold priming to be able to illustrate the increased probability of CSD generation with sensory stimulation. Yet, in 1 out of 7 mice, with photic stimulation and, 1 out of 6 mice, with whisker stimulation, we were able to evoke stimulus-induced CSDs after knockdown. These CSDs were triggered by stimulation as their temporal association suggests because no spontaneous CSDs were observed prior to stimulation or in 6 knockdown mice that were not stimulated but used for KCl-induced CSD threshold experiments. In line with the relatively lower CSD susceptibility created by partial reduction in α2-Na^+/K^+-ATPase mRNA compared to the ouabain-treated group, K^+ rise during whisker stimulation in α2-Na^+/K^+-ATPase knockdown mice significantly increased but to a lesser extent than that observed with low dose ouabain treatment. This can also explain the consistently lower CSD threshold in knockdown mice, in which sub-threshold amounts of exogenously applied KCl can bring the extracellular K^+ levels over the threshold due to partially inefficient uptake as also observed in brain slices obtained from heterozygous α2-Na^+/K^+-ATPase knockout mice [23]. The reduced K^+ uptake during sensory stimulation-induced synaptic activity and susceptibility to CSD were not detected in blank plasmid injected control mice, showing that cortical injection before the experiment did not create the observed susceptibility. Altogether, these data suggest that conditions that reduce/slow down uptake of synaptically released K^+ and glutamate during intense sensory stimulation can increase the probability of CSD generation. In the somatosensory cortex, glutamate uptake by astrocyte processes is slower during sustained synaptic stimulation, which may have increased the CSD incidence during our prolonged photic or whisker stimulation [37]. It has recently been shown that migraine triggers like sleep deprivation, which reduces the availability of glycogen-derived glucose for synaptic metabolism, lowers the CSD threshold likely because the reuptake of K^+ and glutamate largely depends on the glucose liberated from glycogen in astrocyte processes during intense/prolonged neuronal activity [28]. Insufficient fueling of α2-Na^+/K^+-ATPase can cause excess K^+ accumulation during prolonged sensory stimulation as shown here *in vivo* [13, 33, 41]. Therefore, it is likely that migraine triggers can prime the

brain for CSD generation during synaptic activity on a susceptible background by reducing capacity for reuptake of released K^+ and glutamate.

Sensory stimuli as migraine triggers

Migraine attacks can be triggered by a number of physiological and environmental factors. Intense sensory stimuli such as flickering or pulsating lights, bright or reflected sunshine, noise or loud sounds, strong odors are among migraine triggers [6, 7]. Bright light has been reported as a migraine trigger in 28-61 % of the people with migraine with aura [6, 7, 42, 43]. Although a single trigger may set off migraine attack in some migraineurs, a number of endogenous and exogenous factors should come together in order to initiate an attack in most others. Possibly, these factors, when present in combination and/or sufficient intensity, bring a genetically/hormonally susceptible brain of migraineur up to the threshold of CSD initiation. Supporting this view, Cao et al showed that visual stimulation of around 7 minutes triggered their typical headache in 8 out of 12 migraine patients [44]. In 5 of these patients, slowly propagating (at a rate of 3 to 6 mm/min) suppression of the visually evoked MRI-BOLD response in the occipital cortex was observed, in accordance with induction of a CSD. Indeed, this neuronal suppression was accompanied by baseline MRI-BOLD changes reminiscent of the vasodilatation associated with CSD. Sensory cortices including the visual cortex may be more susceptible to CSD possibly due to relatively inefficient potassium and glutamate clearance rates or to the marginally optimal distance between astrocyte processes and excitatory synapses [37, 45]. Taken together, these findings support the hypothesis that intense synaptic activity can trigger CSD in susceptible brain of migraineurs when intrinsic mechanisms to prevent CSD have been surpassed. The probabilistic nature of CSD generation in the primed mouse brain as in migraineurs points to efficient safety mechanisms that limit CSD generation even in the presence of predisposing and priming factors. The safety mechanisms are likely to be multiple, however, adenosine seems to play a significant role. Since adenosine derived from the ATP is a measure of intense synaptic activity, it is ideally situated to prevent uncontrolled hyperactivity and synchronization by reducing glutamate release and postsynaptic excitability in cortex as our findings suggest [46, 47]. A similar role for adenosine was also suggested for prevention of seizure activity [48]. Interestingly, antagonizing A1 subtype adenosine receptors alone was sufficient to induce CSD without any experimental stimulation. Hence, the effect of photic stimulation could only be tested when the A1 antagonism was less efficient. Under these conditions, sensory stimulation caused small-amplitude DC shifts coincident with EEG suppression [24]. These were possibly caused by synchronization of a smaller aggregate of neurons than was required for full-blown CSD, which may have been prevented by the intact glutamate and K^+ uptake not allowing recruitment of more neurons and propagation of depolarization wave. However, when sufficient concentrations of DPCPX were achieved, unregulated release of glutamate may have created glutamate plumes that increase the CSD probability as shown after promoting glutamate release with veratridine [36]. Unfortunately, a finer control over the DPCPX concentration was not feasible because of its poor solubility or significant cardiotoxicity upon its systemic administration, typical limitations of A1 antagonists. GABAA antagonism was not effective in inducing CSD in line with previous literature [1, 3]. However, in one mouse, a CSD was induced during

sensory stimulation; the rise in extracellular K^+ and glutamate caused by bicuculine-induced synchronized discharges coincident with stimulation might have lowered the CSD threshold in this mouse (similar to FHM3 knock-in mouse that exhibit extracellular K^+ build-up and low CSD threshold due to GABAergic interneuron hyperactivity [49, 50]); reinforcing the idea that a significant rise in K^+ and glutamate, rather than reduced GABAergic inhibition are more critical for CSD ignition [1, 3].

In conclusion, our findings suggest that normal brain is well protected against CSD generation. For CSD to be ignited under physiological conditions, several priming and predisposing factors are required as seen in migraine patients. Intense sensory stimulation has the potential to trigger a CSD when co-existing conditions can bring extracellular K^+ and glutamate concentrations over a threshold. Therefore, factors that reduce uptake of K^+ and glutamate released from synapses (e.g. inefficient fueling of α2-Na^+/K^+-ATPase due to reduced glycogen breakdown after sleep deprivation [51]) or facilitate glutamate release (e.g. reduced presynaptic adenosinergic inhibition) similar to mechanisms documented for FHM2 and FHM1 mutations, respectively, may prime the brain for CSD generation with excitatory synaptic activity.

List Of Abbreviations

aCSF: artificial cerebrospinal fluid

Ag-AgCl: silver-silver chloride

APG-4: Asante Potassium Green-4

ATP1A2: ATPase Na+/K+ transporting subunit alpha 2

AUC: area under the curve

BODIPY: boron-dipyrromethene

BOLD: blood oxygenation level dependent

CBF: cerebral blood flow

CCD: charge-coupled device

cDNA: complementary DNA

CSD: cortical spreading depression

DC: direct current

DMSO: dimethyl sulfoxide

DPCPX: 8-cyclopentyl-1,3-dipropylxanthine

FHM2: familial hemiplegic migraine-2

GAPDH: glyceraldehyde 3-phosphate dehydrogenase

IPG-4: ION Potassium Green-4

KCl: potassium chloride

LED: light emitting diode

Na^+/K^+-ATPase: sodium potassium pump

qRT-PCR: quantitative reverse transcription polymerase chain reaction

ROI: region of interest

shRNA: short harpin RNA

Declarations

Ethics approval

All animal experiments were performed in accordance with relevant guidelines and regulations, and were approved by Hacettepe University Animal Experiments Ethics Committee (2012/53-01, 2017/05-2).

Consent for publication

Not applicable

Availability of data and materials

The datasets used and/or analysed during the current study are available from the corresponding author on reasonable request.

Competing interests

The authors declare that they have no competing interests

Funding

This study was supported by grants from The Scientific and Technological Research Council of Turkey (TÜBİTAK-113S211) and Hacettepe University Scientific Research Projects Unit (014-D01-105-002).

Authors' contributions

T.D. designed the study. S.H., and A.T.S. performed experiments and analyzed the data. H.K., B.D.D., S.Y.O. and E.E.K. performed experiments. H.K., E.E.K, Y.G.O. and T.D. supervised the project. T.D. and S.H. drafted the manuscript. All authors critically revised and have approved the submitted version of the manuscript.

Acknowledgements

The authors thanks to Drs. Kıvılcım Kılıç, Murat Yılmaz, Berkan Kaplan and Anisa Dehghani Mohammadi for their help with the experiments, Dr. Nurhan Erbil for helping in Matlab scripts, Dr. Gokhan Uruk for his assistance in fluorescent signal analysis, Mesut Firat for technical support, and, to Prof. Muge Yemisci for comments on the poster presentation at SFN, to Dr. Gilbert Gallardo for providing plasmid expressing α2-Na^+/K^+-ATPase-shRNA.

References

1. Pietrobon D, Moskowitz MA (2014) Chaos and commotion in the wake of cortical spreading depression and spreading depolarizations. Nat Rev Neurosci 15:379–393. https://doi.org/10.1038/nrn3770
2. Ayata C, Lauritzen M (2015) Spreading Depression, Spreading Depolarizations, and the Cerebral Vasculature. Physiol Rev 95:953–993. https://doi.org/10.1152/physrev.00027.2014
3. Somjen GG (2001) Mechanisms of spreading depression and hypoxic spreading depression-like depolarization. Physiol Rev 81:1065–1096. https://doi.org/10.1152/physrev.2001.81.3.1065
4. Houben T, Loonen IC, Baca SM, et al (2017) Optogenetic induction of cortical spreading depression in anesthetized and freely behaving mice. J Cereb Blood Flow Metab 37:1641–1655. https://doi.org/10.1177/0271678X16645113
5. Harle DE, Shepherd AJ, Evans BJW (2006) Visual stimuli are common triggers of migraine and are associated with pattern glare. Headache 46:1431–1440. https://doi.org/10.1111/j.1526-4610.2006.00585.x
6. Hauge AW, Kirchmann M, Olesen J (2011) Characterization of consistent triggers of migraine with aura. Cephalalgia 31:416–438. https://doi.org/10.1177/0333102410382795
7. Hoffmann J, Recober A (2013) Migraine and triggers: post hoc ergo propter hoc? Curr Pain Headache Rep 17:370. https://doi.org/10.1007/s11916-013-0370-7
8. Hougaard A, Amin FM, Amin F, et al (2013) Provocation of migraine with aura using natural trigger factors. Neurology 80:428–431. https://doi.org/10.1212/WNL.0b013e31827f0f10
9. Major S, Petzold GC, Reiffurth C, et al (2017) A role of the sodium pump in spreading ischemia in rats. J Cereb Blood Flow Metab 37:1687–1705. https://doi.org/10.1177/0271678X16639059
10. De Fusco M, Marconi R, Silvestri L, et al (2003) Haploinsufficiency of ATP1A2 encoding the Na+/K+ pump alpha2 subunit associated with familial hemiplegic migraine type 2. Nat Genet 33:192–196. https://doi.org/10.1038/ng1081

11. Leo L, Gherardini L, Barone V, et al (2011) Increased susceptibility to cortical spreading depression in the mouse model of familial hemiplegic migraine type 2. PLoS Genet 7:e1002129. https://doi.org/10.1371/journal.pgen.1002129
12. Kros L, Lykke-Hartmann K, Khodakhah K (2018) Increased susceptibility to cortical spreading depression and epileptiform activity in a mouse model for FHM2. Sci Rep 8:16959. https://doi.org/10.1038/s41598-018-35285-8
13. Isaksen TJ, Lykke-Hartmann K (2016) Insights into the Pathology of the α2-Na(+)/K(+)-ATPase in Neurological Disorders; Lessons from Animal Models. Front Physiol 7:161. https://doi.org/10.3389/fphys.2016.00161
14. Pellerin L, Magistretti PJ (1997) Glutamate uptake stimulates Na+,K+-ATPase activity in astrocytes via activation of a distinct subunit highly sensitive to ouabain. J Neurochem 69:2132–2137. https://doi.org/10.1046/j.1471-4159.1997.69052132.x
15. Stoica A, Larsen BR, Assentoft M, et al (2017) The α2β2 isoform combination dominates the astrocytic Na+ /K+ -ATPase activity and is rendered nonfunctional by the α2.G301R familial hemiplegic migraine type 2-associated mutation. Glia 65:1777–1793. https://doi.org/10.1002/glia.23194
16. Hara K, Harris RA (2002) The anesthetic mechanism of urethane: the effects on neurotransmitter-gated ion channels. Anesth Analg 94:313–318, table of contents. https://doi.org/10.1097/00000539-200202000-00015
17. Kudo C, Nozari A, Moskowitz MA, Ayata C (2008) The impact of anesthetics and hyperoxia on cortical spreading depression. Exp Neurol 212:201–206. https://doi.org/10.1016/j.expneurol.2008.03.026
18. Boroojerdi B, Bushara KO, Corwell B, et al (2000) Enhanced excitability of the human visual cortex induced by short-term light deprivation. Cereb Cortex 10:529–534. https://doi.org/10.1093/cercor/10.5.529
19. Ayata C, Dunn AK, Gursoy-OZdemir Y, et al (2004) Laser speckle flowmetry for the study of cerebrovascular physiology in normal and ischemic mouse cortex. J Cereb Blood Flow Metab 24:744–755. https://doi.org/10.1097/01.WCB.0000122745.72175.D5
20. Brennan KC, Romero Reyes M, López Valdés HE, et al (2007) Reduced threshold for cortical spreading depression in female mice. Ann Neurol 61:603–606. https://doi.org/10.1002/ana.21138
21. Bazzigaluppi P, Dufour S, Carlen PL (2015) Wide field fluorescent imaging of extracellular spatiotemporal potassium dynamics in vivo. Neuroimage 104:110–116. https://doi.org/10.1016/j.neuroimage.2014.10.012
22. von Bornstädt D, Houben T, Seidel JL, et al (2015) Supply-demand mismatch transients in susceptible peri-infarct hot zones explain the origins of spreading injury depolarizations. Neuron 85:1117–1131. https://doi.org/10.1016/j.neuron.2015.02.007
23. Reiffurth C, Alam M, Zahedi-Khorasani M, et al (2020) Na+/K+-ATPase α isoform deficiency results in distinct spreading depolarization phenotypes. J Cereb Blood Flow Metab 40:622–638.

https://doi.org/10.1177/0271678X19833757

24. Lindquist BE, Shuttleworth CW (2017) Evidence that adenosine contributes to Leao's spreading depression in vivo. J Cereb Blood Flow Metab 37:1656–1669. https://doi.org/10.1177/0271678X16650696
25. Dalkara T, Moskowitz MA (2017) From Cortical Spreading Depression to Trigeminovascular Activation in Migraine. In: Neurobiological Basis of Migraine. John Wiley & Sons, Ltd, pp 267–284
26. Karatas H, Erdener SE, Gursoy-Ozdemir Y, et al (2013) Spreading depression triggers headache by activating neuronal Panx1 channels. Science 339:1092–1095. https://doi.org/10.1126/science.1231897
27. Bolay H, Reuter U, Dunn AK, et al (2002) Intrinsic brain activity triggers trigeminal meningeal afferents in a migraine model. Nat Med 8:136–142. https://doi.org/10.1038/nm0202-136
28. Kilic K, Karatas H, Dönmez-Demir B, et al (2018) Inadequate brain glycogen or sleep increases spreading depression susceptibility. Ann Neurol 83:61–73. https://doi.org/10.1002/ana.25122
29. Balestrino M, Young J, Aitken P (1999) Block of (Na+,K+)ATPase with ouabain induces spreading depression-like depolarization in hippocampal slices. Brain Res 838:37–44. https://doi.org/10.1016/s0006-8993(99)01674-1
30. Blanco G, Mercer RW (1998) Isozymes of the Na-K-ATPase: heterogeneity in structure, diversity in function. Am J Physiol 275:F633-650. https://doi.org/10.1152/ajprenal.1998.275.5.F633
31. Calderon DP, Fremont R, Kraenzlin F, Khodakhah K (2011) The neural substrates of rapid-onset Dystonia-Parkinsonism. Nat Neurosci 14:357–365. https://doi.org/10.1038/nn.2753
32. Tang YT, Mendez JM, Theriot JJ, et al (2014) Minimum conditions for the induction of cortical spreading depression in brain slices. J Neurophysiol 112:2572–2579. https://doi.org/10.1152/jn.00205.2014
33. Capuani C, Melone M, Tottene A, et al (2016) Defective glutamate and K+ clearance by cortical astrocytes in familial hemiplegic migraine type 2. EMBO Mol Med 8:967–986. https://doi.org/10.15252/emmm.201505944
34. Cholet N, Pellerin L, Magistretti PJ, Hamel E (2002) Similar perisynaptic glial localization for the Na+,K+-ATPase alpha 2 subunit and the glutamate transporters GLAST and GLT-1 in the rat somatosensory cortex. Cereb Cortex 12:515–525. https://doi.org/10.1093/cercor/12.5.515
35. Grewer C, Rauen T (2005) Electrogenic glutamate transporters in the CNS: molecular mechanism, pre-steady-state kinetics, and their impact on synaptic signaling. J Membr Biol 203:1–20. https://doi.org/10.1007/s00232-004-0731-6
36. Parker PD, Suryavanshi P, Melone M, et al (2021) Non-canonical glutamate signaling in a genetic model of migraine with aura. Neuron 109:611-628.e8. https://doi.org/10.1016/j.neuron.2020.11.018
37. Romanos J, Benke D, Saab AS, et al (2019) Differences in glutamate uptake between cortical regions impact neuronal NMDA receptor activation. Commun Biol 2:127. https://doi.org/10.1038/s42003-019-0367-9

38. Hunanyan AS, Fainberg NA, Linabarger M, et al (2015) Knock-in mouse model of alternating hemiplegia of childhood: behavioral and electrophysiologic characterization. Epilepsia 56:82–93. https://doi.org/10.1111/epi.12878
39. Panagiotakaki E, De Grandis E, Stagnaro M, et al (2015) Clinical profile of patients with ATP1A3 mutations in Alternating Hemiplegia of Childhood-a study of 155 patients. Orphanet J Rare Dis 10:123. https://doi.org/10.1186/s13023-015-0335-5
40. Schlingmann KP, Bandulik S, Mammen C, et al (2018) Germline De Novo Mutations in ATP1A1 Cause Renal Hypomagnesemia, Refractory Seizures, and Intellectual Disability. Am J Hum Genet 103:808–816. https://doi.org/10.1016/j.ajhg.2018.10.004
41. Xu J, Song D, Xue Z, et al (2013) Requirement of glycogenolysis for uptake of increased extracellular K+ in astrocytes: potential implications for K+ homeostasis and glycogen usage in brain. Neurochem Res 38:472–485. https://doi.org/10.1007/s11064-012-0938-3
42. Kelman L (2007) The triggers or precipitants of the acute migraine attack. Cephalalgia 27:394–402. https://doi.org/10.1111/j.1468-2982.2007.01303.x
43. Peroutka SJ (2014) What turns on a migraine? A systematic review of migraine precipitating factors. Curr Pain Headache Rep 18:454. https://doi.org/10.1007/s11916-014-0454-z
44. Cao Y, Welch KM, Aurora S, Vikingstad EM (1999) Functional MRI-BOLD of visually triggered headache in patients with migraine. Arch Neurol 56:548–554. https://doi.org/10.1001/archneur.56.5.548
45. Bogdanov VB, Middleton NA, Theriot JJ, et al (2016) Susceptibility of Primary Sensory Cortex to Spreading Depolarizations. J Neurosci 36:4733–4743. https://doi.org/10.1523/JNEUROSCI.3694-15.2016
46. Cunha RA (2005) Neuroprotection by adenosine in the brain: From A(1) receptor activation to A (2A) receptor blockade. Purinergic Signal 1:111–134. https://doi.org/10.1007/s11302-005-0649-1
47. Qi G, van Aerde K, Abel T, Feldmeyer D (2017) Adenosine Differentially Modulates Synaptic Transmission of Excitatory and Inhibitory Microcircuits in Layer 4 of Rat Barrel Cortex. Cereb Cortex 27:4411–4422. https://doi.org/10.1093/cercor/bhw243
48. Masino SA, Kawamura M, Ruskin DN (2014) Adenosine receptors and epilepsy: current evidence and future potential. Int Rev Neurobiol 119:233–255. https://doi.org/10.1016/B978-0-12-801022-8.00011-8
49. Jansen NA, Dehghani A, Linssen MML, et al (2020) First FHM3 mouse model shows spontaneous cortical spreading depolarizations. Ann Clin Transl Neurol 7:132–138. https://doi.org/10.1002/acn3.50971
50. Chever O, Zerimech S, Scalmani P, et al (2020) GABAergic neurons and Na_V 1.1 channel hyperactivity: a novel neocortex-specific mechanism of Cortical Spreading Depression. Neuroscience
51. Petit J-M, Eren-Koçak E, Karatas H, et al (2021) Brain glycogen metabolism: A possible link between sleep disturbances, headache and depression. Sleep Med Rev 59:101449. https://doi.org/10.1016/j.smrv.2021.101449

Table

Table 1. CSD onset latency and frequency with different concentrations of topical ouabain application in the mouse brain (total volume for each animal equals to 5 uL in all experiments). (none: no CSD detected, rare: 1-2 CSDs/h, frequent: ≥3 CSDs/h)

Concentration (mM)	Latency to CSD onset (min) (mean±SE)	Latency to CSD onset (min) (range)	CSD pattern (frequency)
0.1	46.3±4.4	6 - 68	% 25 none % 50 rare % 25 frequent
0.15	40.2±4.2	14 - 68	% 20 none % 28 rare % 52 frequent
0.3	20.7±5.6	6 - 33	%100 frequent
1	13.2±2.5	7 - 14	%100 frequent

Figures

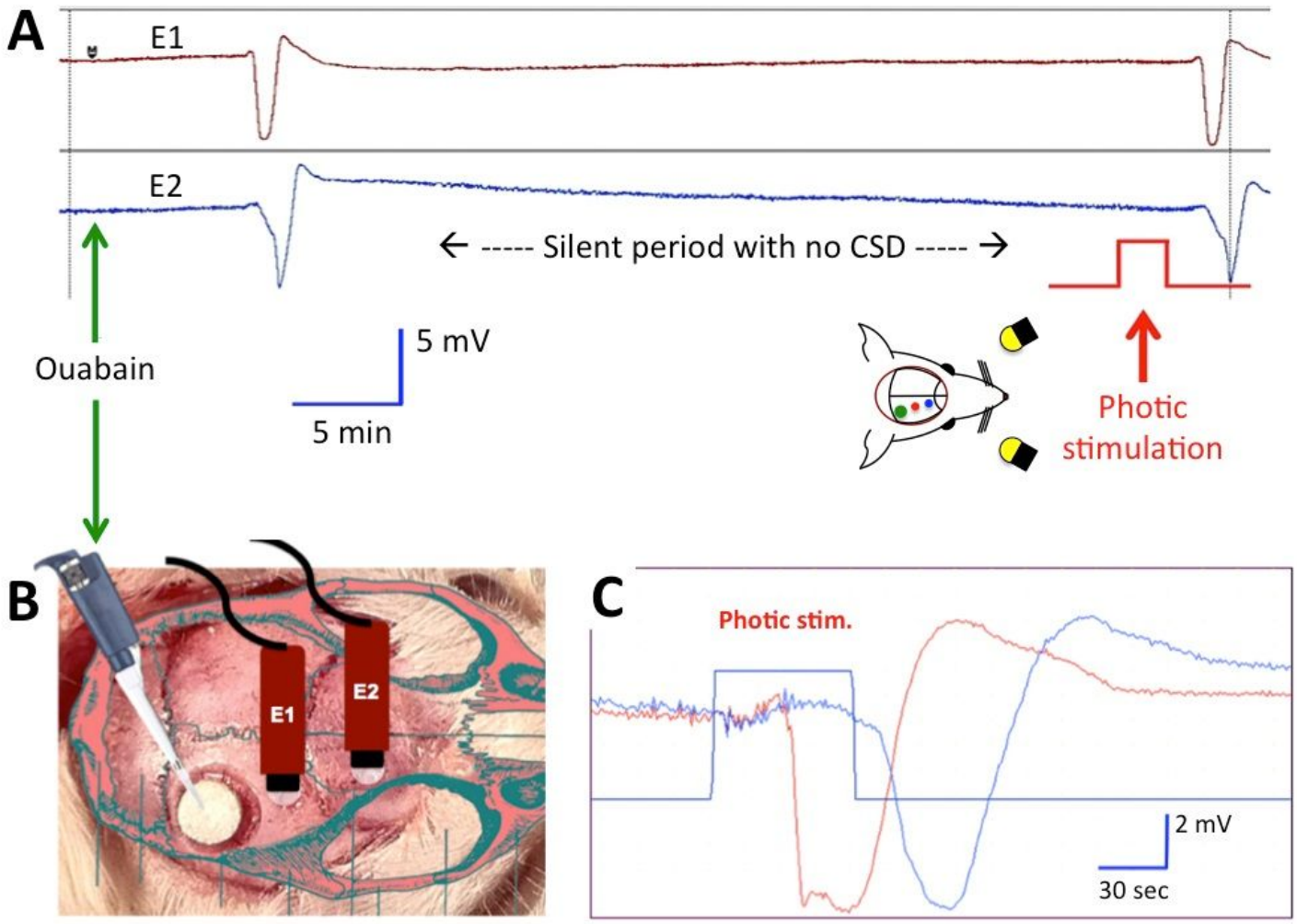

Figure 1

Photic stimulation evokes CSD in the visual cortex primed with around-the threshold dose of ouabain. A) shows the DC potential recordings from 2 extracranial electrodes placed 1 mm apart anterior to the cranial window opened over the occipital cortex. Ouabain (0.1 mM) application over the dura induced a single CSD. After a silent period of 30 min without any CSD, photic stimulation (1 min at 12 Hz) evoked a CSD in this mouse. B) illustrates the placement of electrodes and cranial window over the mouse skull as also depicted at the bottom of A. C) shows another example of CSD evoked with photic stimulation. The distance between CSD generating primed occipital cortex area and recording electrodes causes the latency between the photic stimulation pulse and DC shifts.

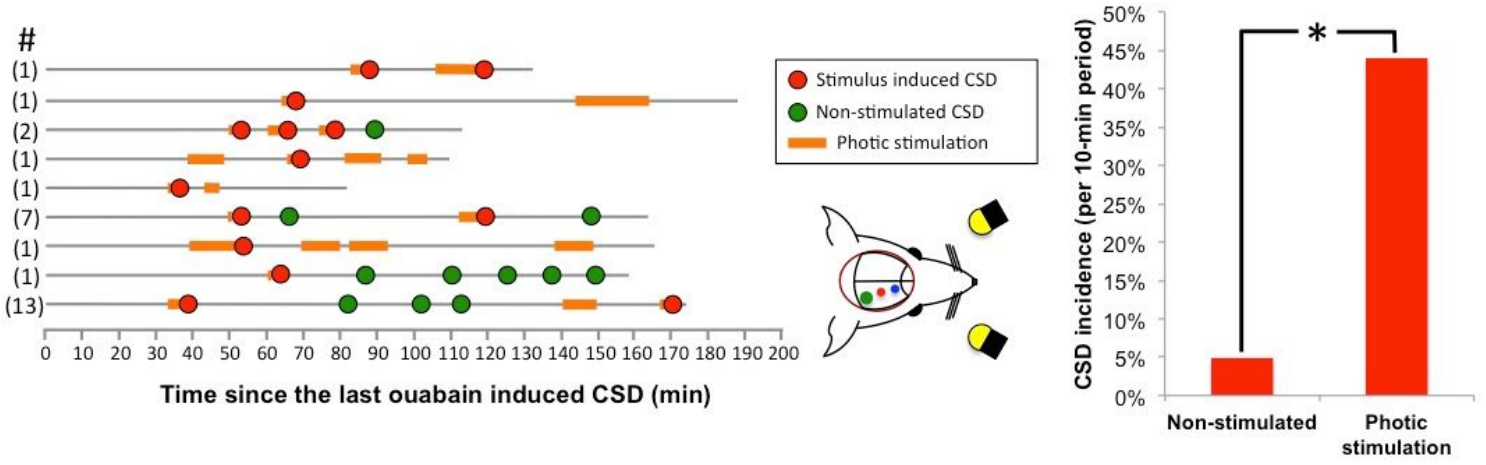

Figure 2

Priming the occipital cortex with ouabain increased the incidence of photic stimulation-induced CSDs. Each horizontal line represents continuous recording from one mouse primed with 0.1 mM ouabain and then subjected to 1-min on and off cycles of photic stimulation at 8-12 Hz. Stimulation started after at least a 30-min silent period without any CSD. The number of ouabain-induced CSDs prior to starting stimulation is given before each line. Stimulation cycles (labeled orange) were stopped when a CSD was triggered (red circles). Green circles depict the occasional CSDs unrelated to stimulation. Bar graph shows that the CSD incidence was significantly higher (*p 0.001, Chi-square test) during photic stimulation compared to the non-stimulated periods.

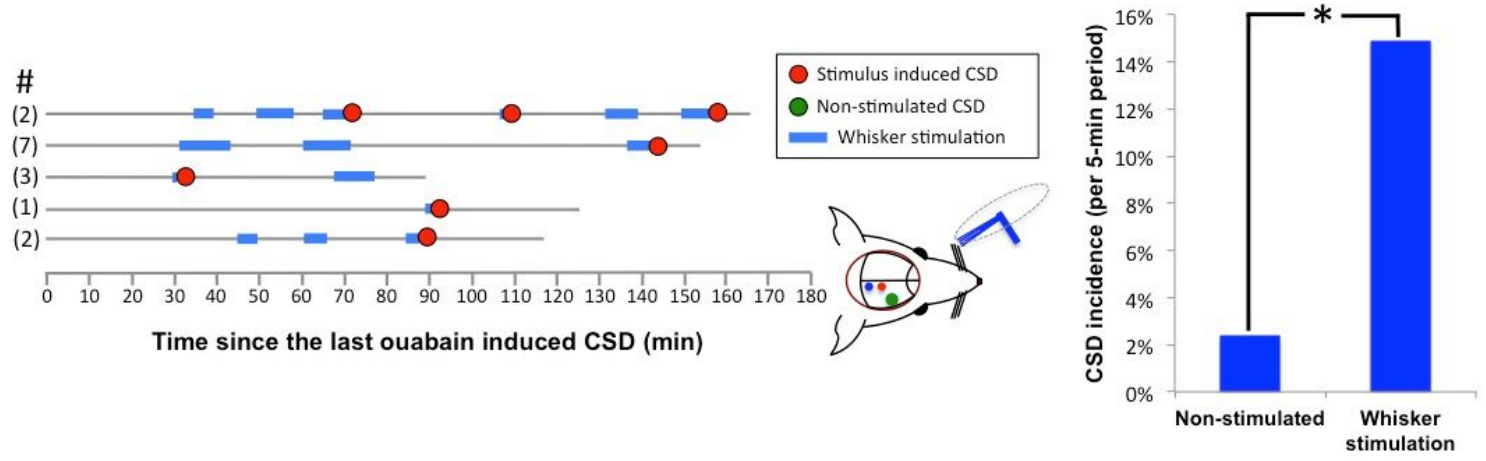

Figure 3

Priming the barrel cortex with ouabain increased the incidence of whisker stimulation-induced CSDs. Each horizontal line represents continuous recording from one mouse primed with 0.1 mM ouabain and then subjected to whisker stimulation at 8-12 Hz. Stimulation started after at least a 30-min silent period without any CSD. The number of ouabain-induced CSDs prior to starting stimulation is given before each line. Stimulation periods (labeled blue) were stopped when a CSD was triggered (red circles). Green circles

depict the occasional CSDs unrelated to stimulation. Bar graph shows that the CSD incidence was significantly higher (*p=0.026, Chi-square test) during photic stimulation compared to the non-stimulated periods.

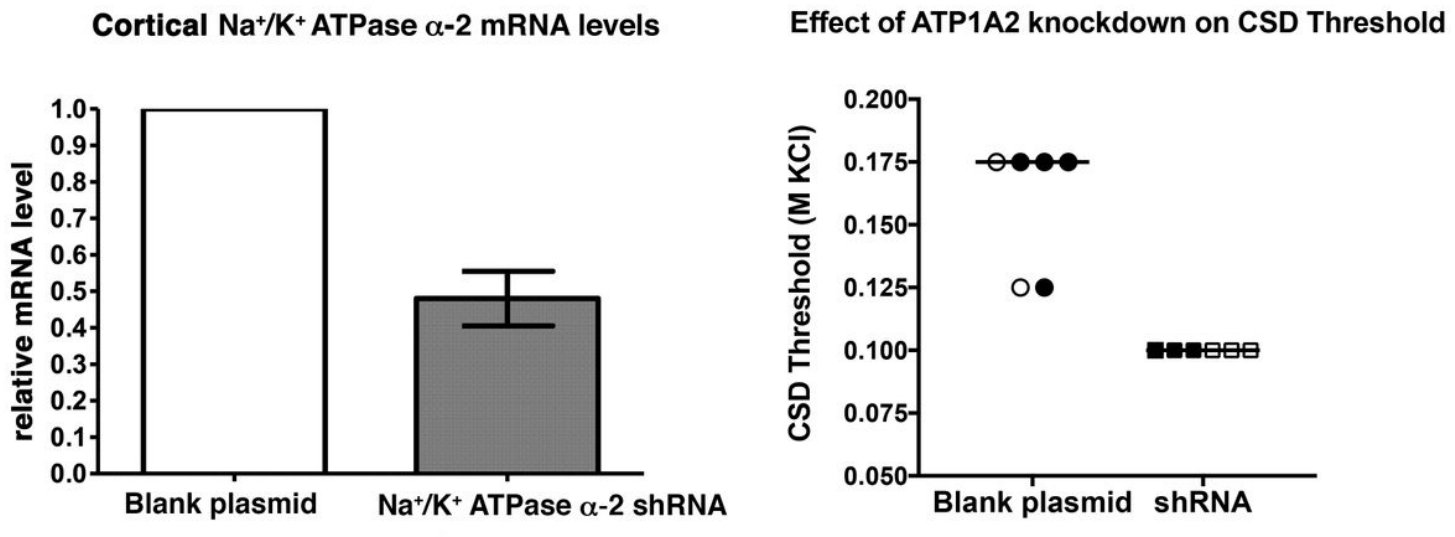

Figure 4

Knocking down cortical α2-Na+/K+-ATPase lowered the CSD threshold. Intracortical injection of α2-Na+/K+-ATPase shRNA-coding plasmids to the occipital cortex led to a 50 % decrease in α2-Na+/K+-ATPase mRNA level as detected by qRT-PCR (left, p=0.07, unpaired t-test) and reduced the CSD induction threshold (right) as assessed with varying concentrations of KCl (from 0.050 to 0,175 M) 6 (clear symbols) or 24 hours (filled symbols) after injection compared to the blank plasmid-injected group (median= 0.1 M KCl vs 0.175 M KCl, p=0.002, Mann-Whitney U test).

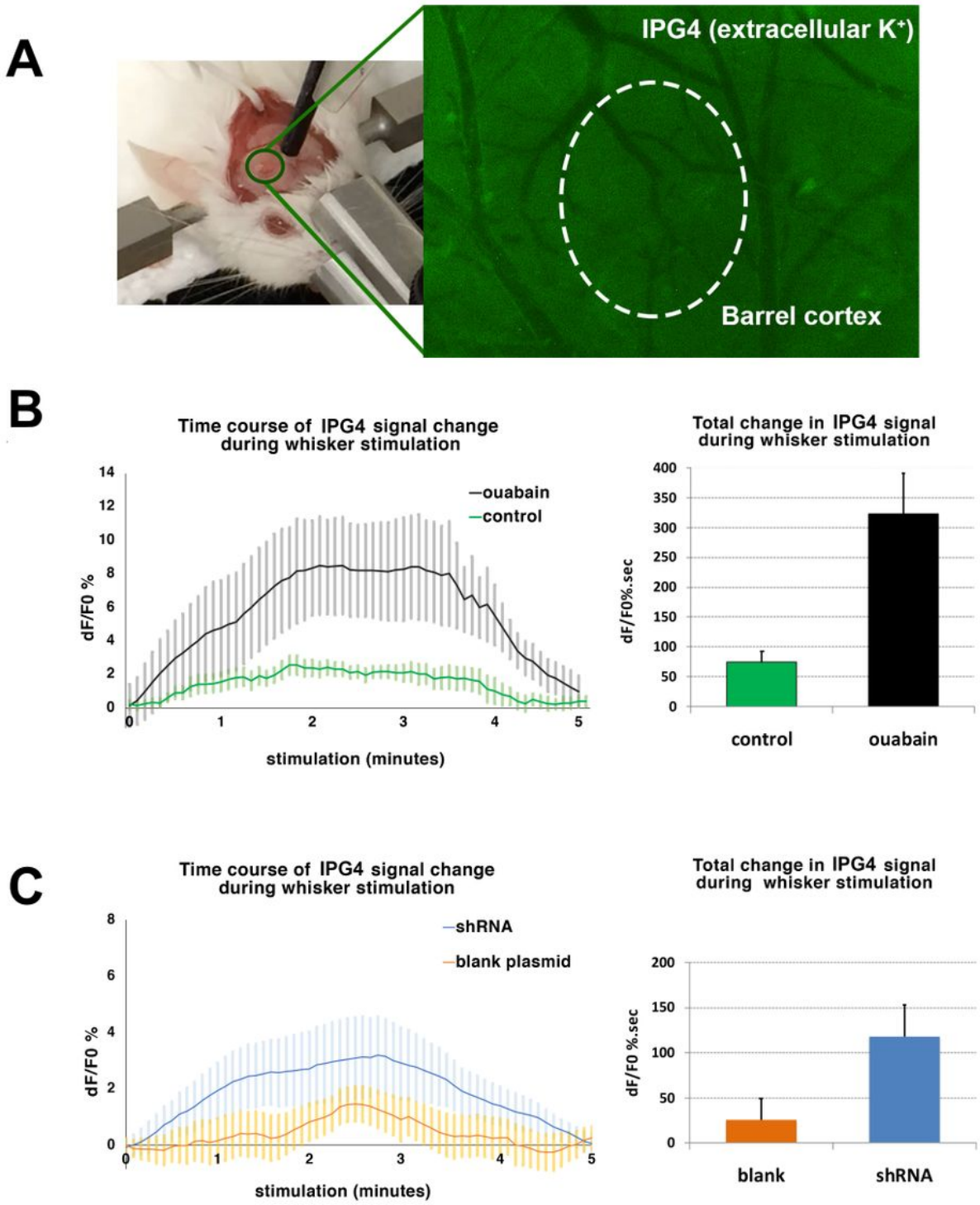

Figure 5

α2-Na+/K+-ATPase knockdown or ouabain reduced K+ uptake during whisker stimulation. In order to investigate the extracellular potassium changes, a fluorescent potassium probe, Asante Potassium Green-4 (IPG-4) was used. A) The potassium sensitivity of IPG-4 fluorescence was linear within the range encountered in the extracellular space during CSD as assessed in vitro. B and C) We monitored the extracellular potassium changes through a cranial window placed over the barrel cortex (picture) by

plotting the relative fluorescence intensity change (dF/F0) over time (graphs on the left) and calculating the area under the curve (bars on the right). In ouabain-primed (0.1 mM) cortex, 5 min of 10 Hz whisker stimulation resulted in a significant increase in potassium fluorescence compared to aCSF-treated control group (n=6 mice for each group)(p=0.004, Mann-Whitney U test). Similarly, there was significant increase in potassium signal during whisker stimulation in α2-Na+/K+-ATPase shRNA-encoding plasmid injected mice compared to blank plasmid injected animals (p=0.055, Mann-Whitney U test). Error bars represent SEM.

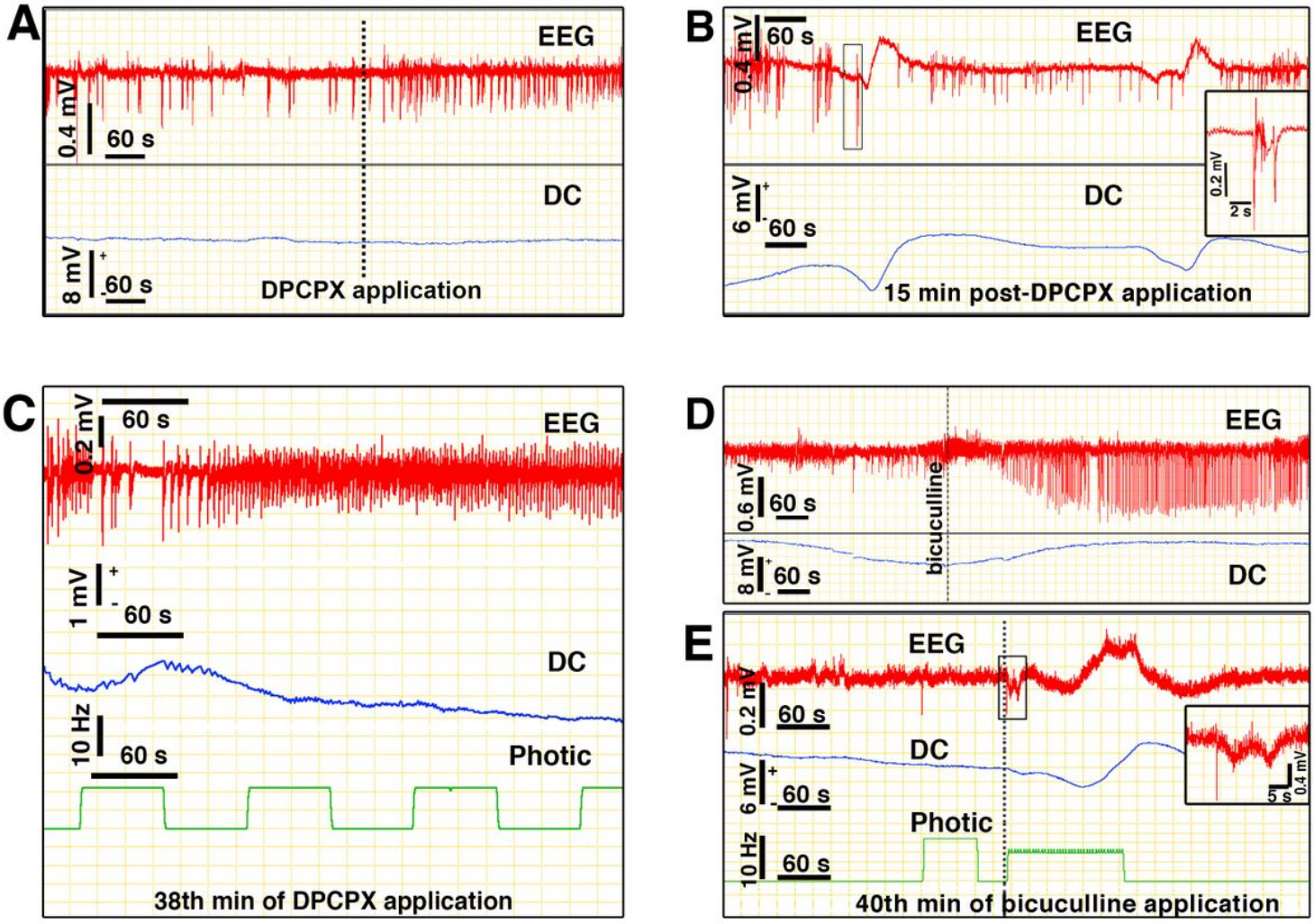

Figure 6

Adenosine generated during synaptic activity may be one of the safety mechanisms preventing CSD ignition. A) Epidurally applied selective A1-receptor antagonist, DPCPX (1 mM) induced irregularly spaced synchronized discharges, indicating that it sufficiently penetrated cortex. B) DPCPX applied to the non-primed occipital cortex caused full-blown CSDs without stimulation in 4 out of 8 mice, whereas photic stimulation evoked a small-DC shift during which ongoing EEG activity (except large-amplitude synchronized discharges) was suppressed during 10 out of 116 photic stimulation periods (C). Please note that recordings were obtained with extracranial electrodes so, they also pick-up activity from the cortex surrounding the focus generating the CSD-like wave. The EEG suppression was not caused by

stimulation, as the following stimulation periods did not affect the EEG activity. D) Epidurally applied GABAA antagonist bicuculline (10 mM) consistently induced irregularly spaced synchronized discharges, ensuring that it sufficiently penetrated cortex. The small concave DC potential change is an artifact induced during the setting up the cranial window for bicuculline application unlike the DC shift in C, where DPCPX application took place 38 minutes ago. D) Bicuculine applied over the occipital cortex triggered a full-blown CSD during photic stimulation in only one out of six mice. Note that high gain EEG recordings shown with an expanded time scale disclose a high amplitude discharge just before CSDs, possibly corresponding the neuronal synchronization preceding CSD generation (insets in B and D).